Structure in liquid water: A study of spatial distribution functions

I. M. Svishchev and P. G. Kusalik
Department of Chemistry, Dalhousie University, Halifax, Nova Scotia, B3H 4J3, Canada

(Received 3 March 1993; accepted 3 May 1993)

Despite the fact that an enormous literature has now accumulated on the structure in liquid water, the focus has been primarily limited to the average radial distributions of particles; local (atomic) pair-density maps which span both the radial and the angular coordinates of the separation vector have remained largely unexplored. In this work, we have obtained the spatial distribution functions $g_{OO}(r,\Omega)$ and $g_{OH}(r,\Omega)$ for liquid water and have applied them to an analysis of the equilibrium structure. Molecular dynamics simulations of SPC/E water have been carried out at temperatures of -10, 25, and 100 °C and the local liquid structure examined. It is found that the unfolded O···O distribution demonstrates, in addition to peaks consistent with a continuous tetrahedral network pattern, a distinct maximum in the local atomic pair density at "interstitial" separations of about 3.5 Å. This local maximum is lost in the spatially folded radial distribution function $g_{OO}(r)$ due to averaging over the entire angular space. By examining the peaks in $g_{OO}(r,\Omega)$ due to nearest neighbors, we have shown that the tetrahedral network coordination number in liquid SPC/E water equals 4.0 and does not depend on temperature. The average number of molecules in additional nontetrahedral coordination, which is found to vary with temperature, has also been extracted, enabling us to establish full average coordination numbers of 4.8–5.0 in the temperature range of -10–100 °C. In addition, we have determined and analyzed statistical distributions for the pair energies and H-bond angles for different water fractions as identified from $g_{OO}(r,\Omega)$ and $g_{OH}(r,\Omega)$.

I. INTRODUCTION

In view of its fundamental role in nature, liquid water continues to be a focus of major research attention. Its unusual properties, both under normal and critical conditions, have been intensively studied with physical experiments as well as with computer simulations.[1] Enormous theoretical efforts have also gone into developing models of water and aqueous systems.[1,2] Nevertheless, many principal questions still remain in dispute, especially those touching on the structure in liquid water. Mindful of the long and well-documented history of this subject,[2] one can easily find numerous (and frequently conflicting) approaches to describe water structure; to illustrate current research interest in this area, we refer to a concept of bifurcated hydrogen (H) bonds[3] and to an analysis of five-coordinated fragments which are believed to exist in liquid water.[4]

The structural analysis of water and aqueous solutions presented in the existing literature has dealt primarily with the *orientationally averaged* (or spatially folded) radial distribution functions (RDFs) of atoms, i.e., $g_{OO}(r)$, $g_{OH}(r)$, and $g_{HH}(r)$, which are the usual output of computer simulations and diffraction studies (Vol. 1 of Ref. 1 and Ref. 5). Although these correlation functions reflect many key features of the short-range order in molecular liquids, it should be realized that an average spatial assembly of nonspherical particles cannot be uniquely characterized from these one-dimensional RDFs. Thus, structural models postulated for the molecular ordering in nonsimple liquids based only on one-dimensional RDF will always be somewhat ambiguous. In the case of water, the limited resolution of $g_{OO}(r)$ in the region of the *first minimum* has provoked a long-standing debate (Vol. 1 of Ref. 1 and Ref. 2) on whether the local (molecular) pair density in water at interparticle separations of about 3.5 Å originates from large fluctuations in the separation of first H-bonded neighbors, or from indirect second-neighbor correlations in small four- and five-membered H-bonded rings, or from the distinct so called "interstitial" fraction of water molecules, etc.

Obviously, greater clarity in the structural analysis of molecular liquids could be obtained by utilizing distribution functions which span *both* the radial and angular coordinates of the separation vector. Such orientational-dependent pair-distribution functions proved particularly informative in our recent work with nonequilibrium Coulombic systems.[6] In this study, we were able to characterize, by means of spatially unfolded RDFs, the breakdown of spherical symmetry in the distribution of charged particles around an ion moving in the flow generated by an applied electrical field. However, to our knowledge, no one has yet considered such functions for liquid water.

In the present study, we have employed molecular dynamics (MD) simulations of SPC/E water in order to examine these *spatial distribution functions* (SDFs), namely, $g_{OO}(r,\Omega)$ and $g_{OH}(r,\Omega)$. We have then applied them to the analysis of the local equilibrium structure in this liquid at temperatures of -10, 25, and 100 °C. The results reveal the remarkable sensitivity of $g_{OO}(r,\Omega)$ and $g_{OH}(r,\Omega)$ to the structural transformations in liquid water. (Nonequilibrium SDFs for liquid water subject to alternating electrical fields and their link to dynamics in this system will be analyzed in a future article.[7])

This work can also be viewed as an attempt to reconcile, on a more statistically sound basis, the descriptions of

 0021-9606/93/99(4)/3049/10/$6.00

structural properties of water and aqueous solutions provided by computer simulations and model approaches. Historically, model approaches, which have primarily focused on the oxygen–oxygen radial distribution function $g_{OO}(r)$ have made major contributions to our understanding of water structure. Bernal and Fowler were the first to realize that the short-range order in water is consistent with a tetrahedral packing pattern in the distribution of oxygen atoms.[8] Later, in their classical experimental study of the x-ray diffraction from liquid water, Morgan and Warren[9] suggested that the first coordination shell in water might contain molecules in addition to those located at tetrahedral positions[9] in order to explain the apparent elevated level of molecular density at separations corresponding to the first minimum in $g_{OO}(r)$ ($\sim$3.5 Å). This idea has been developed in detail by Samoilov,[10,11] and Narten, Danford, and Levy[11,12] into the interstitial model for water structure. The interstitial model described liquid water as an equilibrium mixture of two fractions, a fraction with the structure of a three dimensional H-bonded network similar to that of the ice I_h, and a fraction of interstitial molecules occupying the cavities in the ice-like framework (in ice I_h, each molecule in the lattice is 3.47 Å from six cavity centers). Unlike network molecules, the interstitial molecules were assumed to be nonhydrogen bonded. Applications of the interstitial model to studies of electrolyte and nonelectrolyte solutions have been numerous and are described elsewhere.[1,2,10]

Another approach to the structural analysis of liquid water originates with Pople. Starting with an electrostatic description for H bonding (Lennard-Jones and Pople[13]), he introduced the concept of H-bond flexibility.[14] Later, Rice and co-workers (Vol. 7 of Ref. 1 and Ref. 15) considerably improved the descriptive properties of the original Pople model, which has now become known as the continuous random network model (RNM). Unlike mixture models, the RNM accounts for the behavior of $g_{OO}(r)$ at r=3.2–4.0 Å primarily by allowing large fluctuations in H-bond lengths and angles. It is interesting to note that in the RNM, the peak in $g_{OO}(r)$ due to the first neighbor is not symmetric in the interparticle separation, rather it is skewed toward larger separation. The RNM also guarantees that remote (second and third) neighbors have a nonzero probability of being found at separations corresponding to the first minimum in $g_{OO}(r)$. Comparing the RNM with the interstitial model, one could say that, in essence, the RNM postulates an elevated molecular pair density at $r\approx$3.3–3.5 Å more as a specific feature of the continuous network rather than as a fingerprint of a distinct structural fraction.

It is widely believed that computer simulation results generally support one-state type models such as the RNM (Vol. 7 of Ref. 1 and Ref. 16). Indeed, the energy distribution of hydrogen-bonded molecular pairs has a single well-defined maximum, as do the distributions of bond lengths and angles; the oxygen–oxygen RDF exhibits a smooth minimum at separations between 3.2–4.0 Å.[17,18] Shoulders in the statistical distributions at small H-bond energy and angle values are usually interpreted as a result of distortions in the network geometry. [From a topological point of view, network distortions enable H-bonded molecules to form rings of different sizes and geometries, and hence the RNM can also be reformulated on the basis of rings statistics (Vol. of Ref. 7).] However, our study based on an analysis of the SDF yields a richer and more complex picture than can be provided by a distorted tetrahedral network. Our spatially unfolded RDF, $g_{OO}(r,\Omega)$, clearly indicates (in addition to a continuous network pattern) the existence of a separate *maximum* in the local density at interstitial distances (3.2–4.4 Å) and confined to a relatively small region in the orientational subspace Ω. This maximum is lost in the spatially folded (angle-averaged) RDF $g_{OO}(r)$, but is clearly resolved in $g_{OO}(r,\Omega)$.

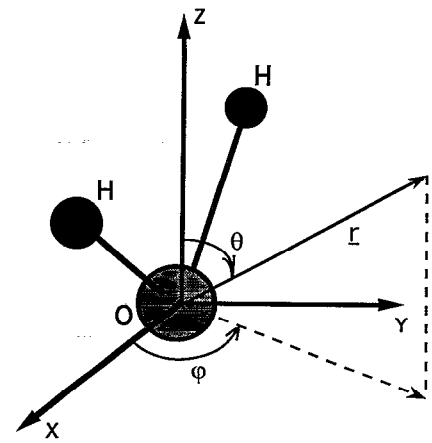

FIG. 1. The principal frame coordinates. Note that the plane of the molecule lies in the XZ plane.

In order to explore further the structural origin of the additional maximum at the separations of 3.2–4.4 Å, a statistical analysis of pair energies and OH$\cdots$O angles has been performed for different types of neighbors [as identified in the $g_{OO}(r,\Omega)$]. Our simulation results indicate that in liquid water, neighboring molecules can be part of the H-bonded network or can be part of a distinct interstitial fraction. We have found that the interstitial molecules can interact strongly with the central water molecule, the average dimerization energy being slightly higher (smaller in magnitude) than the usual threshold energy for a H bond.

The remainder of this paper is organized as follows: In Sec. II, we outline the simulation procedure used in our study and in Sec. III we summarize the simulation results. Section IV is devoted to a detailed discussion of the local structure in liquid SPC/E water. Finally, our conclusions are given in Sec. V.

II. SIMULATION METHODOLOGY

In this article, we report results from MD simulations of liquid water performed with the SPC/E effective pair potential.[19] We recall that in the SPC/E model, each water molecule (shown in Fig. 1) contains three charged sites, a charge of $-0.8476e$ on the oxygen center and two charges of $+0.4238e$ (representing the hydrogens) placed tetrahe-

drally at distances of 1.0 Å from the oxygen site. The single Lennard-Jones site of this model is centered on the oxygen position and is characterized by the parameters of ϵ_{LJ} $=0.6517$ kJ/mol and $\sigma=3.166$ Å.

Our MD simulations have been carried out at constant density and temperature with samples of 108 molecules at temperatures of -10, 25, and 100 °C. Test calculations were also conducted with 256 particles at 25 °C and no system size dependence in the values of $g_{OO}(r,\Omega)$ and $g_{OH}(r,\Omega)$, our major source of structural information, was detected. The influence of a sample size on the thermodynamic and dielectric properties of SPC/E water will be analyzed in detail in a future article.[20] Isothermal conditions were maintained throughout with a Gaussian thermostat[21] and we have chosen to work at experimental densities. In our calculations, we have utilized truncated octahedral geometry for the simulation cell[22] and periodic boundary conditions.[23,24] The Ewald summation technique was used to evaluate the long-range Coulombic forces.[23] In our implementation of this technique, the real space sum was carried over all nearest images, the Fourier space sum was truncated after the first 395 independent lattice vectors (corresponding to $n^2 \leqslant 53$), and the value of the unitless convergence parameter κ was 6.4. The reaction field contribution due to the surrounding dielectric continuum was calculated from the corresponding relationship given elsewhere[23,24]; the dielectric constant of the continuum boundary was taken to be that of real water at the temperature of interest. The Lennard-Jones interactions were truncated spherically at a cutoff of $(\sqrt{3}/4)L$, where L is the length of the cube containing the truncated octahedron. The isokinetic equations of motion were integrated using a fourth-order Gear algorithm[25] and a time step of 1.25 fs. At each temperature, the system was equilibrated for 0.1 ns and averages were accumulated over the subsequent 0.5 ns. The orientational coordinates of the water particles were expressed in terms of quaternion parameters[23] which enabled us to carry out the required "laboratory frame–local frame" transformations of coordinates in an efficient manner.

The following procedure was adopted in order to extract the SDFs $g_{OO}(r,\Omega)$ and $g_{OH}(r,\Omega)$ from our simulations. At frequent intervals during the simulation run, the local spatial frame of every molecule was decomposed on a large number (usually 200) of radial sectors with a vertex on the oxygen site, and for each sector, the pair distribution of interest (OO or OH) was separately accumulated. In our implementation $\Omega \equiv (\theta,\varphi)$, where θ is the angle between the dipole axis and the separation vector $\mathbf{r}$, and φ is the angle between the principal X axis and the projection of $\mathbf{r}$ onto the XY plane (see Fig. 1). Clearly, $g_{OO}(r,\Omega)$ and $g_{OH}(r,\Omega)$ create *spatial maps of the local atomic density* for liquid water; a remote crystallographic solid-state analog of these distribution functions is an atomic density map for a basic crystallographic cell (Brave lattices). Once generated, the rather large amount of numerical data required to represent $g_{OO}(r,\Omega)$ and $g_{OH}(r,\Omega)$ was immediately transferred to a graphical workstation, where it was "sliced" and visualized.

TABLE I. Basic simulation results for SPC/E water.

T (°C)	ϵ	D (10^5 cm^2/s)	$\langle U \rangle$ (kJ/mol)
-10	112±16	0.96±0.07	−43.6±0.4
25	89±13	2.15±0.15	−41.4±0.4
100	51± 4	6.8 ±0.3	−37.1±0.4

III. BASIC SIMULATION RESULTS

Simulation results for SPC/E water, including the average configurational energy [after correction for a positive self-energy of 5.22 kJ/mol (Ref. 19)], static dielectric constant, and self-diffusion coefficient, obtained with a sample of 108 molecules at temperatures of -10, 25, and 100 °C are given in Table I. The usual angle-averaged RDFs $g_{OO}(r)$ and $g_{OH}(r)$ for SPC/E water at -10 °C can be found in Fig. 2. For all quantities, very good agreement with previous calculations[19,26] was obtained.

Our major structural data, SDFs $g_{OO}(r,\Omega)$ and $g_{OH}(r,\Omega)$, are shown in Figs. 3 and 4, respectively, for liquid SPC/E water at -10 °C. For practical reasons, we have plotted them explicitly as the functions of the interatomic separations r and the angles θ for selected values of the angular variable φ; the angles θ and φ are defined as in

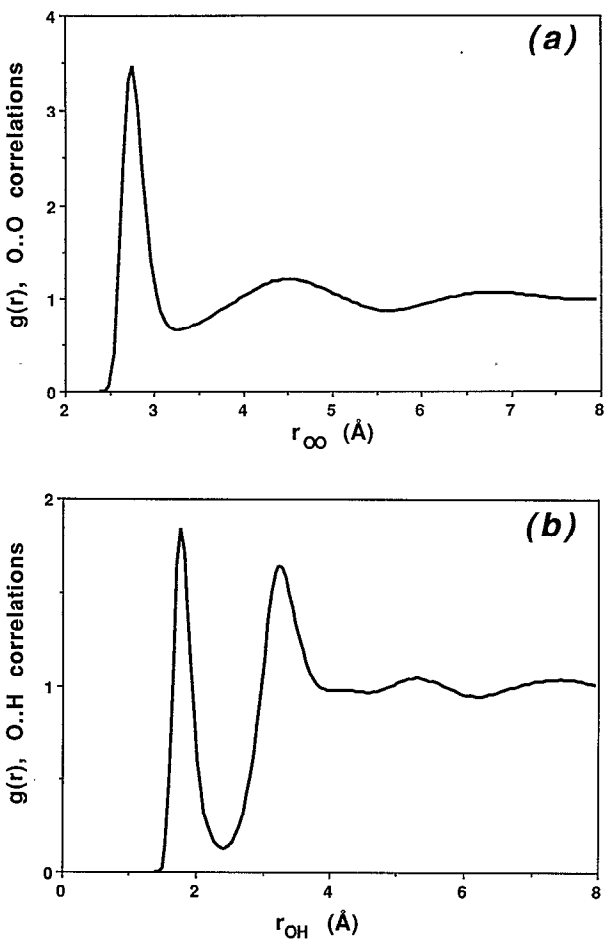

FIG. 2. The radial (or angle-averaged) distribution functions for SPC/E water at -10 °C. (a) $g_{OO}(r)$; (b) $g_{OH}(r)$.

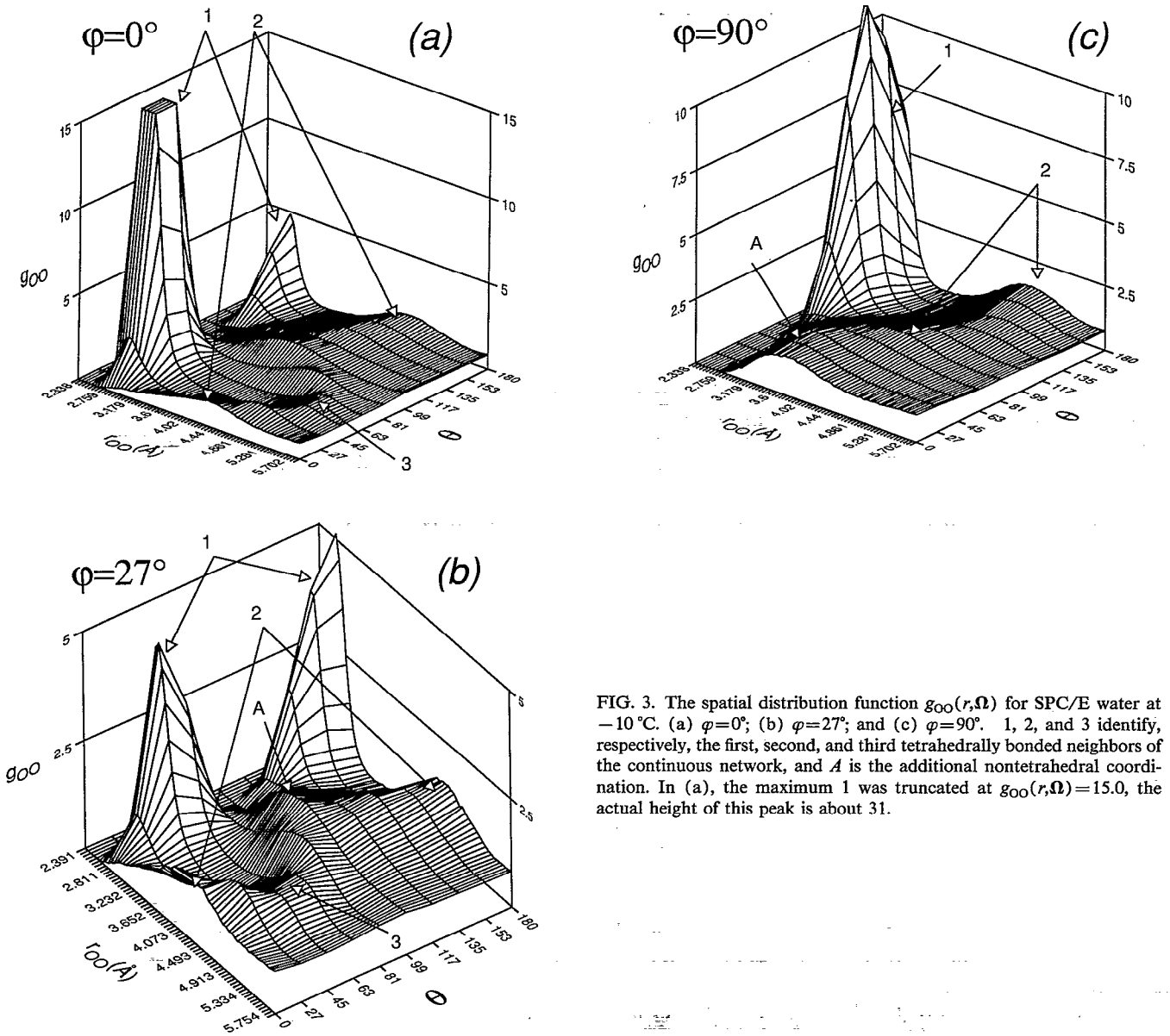

FIG. 3. The spatial distribution function $g_{OO}(r,\Omega)$ for SPC/E water at $-10\,^{\circ}C$. (a) $\varphi=0°$; (b) $\varphi=27°$; and (c) $\varphi=90°$. 1, 2, and 3 identify, respectively, the first, second, and third tetrahedrally bonded neighbors of the continuous network, and A is the additional nontetrahedral coordination. In (a), the maximum 1 was truncated at $g_{OO}(r,\Omega)=15.0$, the actual height of this peak is about 31.

Fig. 1. In Figs. 3(a) and 4(a), slices of $g_{OO}(r,\Omega)$ and $g_{OH}(r,\Omega)$ for $\varphi=0°$ (those in the plane of the H_2O molecule) are shown. In Figs. 3(b) and 4(b), we give $g_{OO}(r,\Omega)$ and $g_{OH}(r,\Omega)$ for $\varphi=27°$, while in Figs. 3(c) and 4(c), we show O···O and O···H correlations in directions perpendicular to the plane of the water molecule. We note that in the latter case of $\varphi=90°$, the directions considered lie in the plane of would-be "lone-pair" electrons of a H_2O molecule. It is obvious from a comparison of the SDFs $g_{OO}(r,\Omega)$ and $g_{OH}(r,\Omega)$ with the usual RDFs $g_{OO}(r)$ and $g_{OH}(r)$ that the former functions convey a great deal more detailed information on the local structure in the liquid.

In order to illustrate temperature variations in the local structure in liquid water, we have also extracted projections of $g_{OO}(r,\Omega)$ at $r=2.71$ Å, the average separation of the first H-bonded neighbors. This function of the angles θ and φ is plotted in Fig. 5 at two different temperatures -10 and $100\,^{\circ}C$.

IV. STRUCTURAL ANALYSIS AND DISCUSSION

A. Interpretation of the structural patterns in $g_{OO}(r,\Omega)$ and $g_{OH}(r,\Omega)$

We begin our structural analysis with an examination of the average local coordination of oxygen atoms in supercooled $T=-10\,^{\circ}C$ liquid water. The appropriate SDF, $g_{OO}(r,\Omega)$ is displayed in different isoangular projections in Fig. 3 and, as we might expect, it reveals predominantly tetrahedral packing of O sites in the local surroundings. For convenience, we have denoted the first, second, and third tetrahedrally packed neighbors, respectively, as 1, 2, and 3 in Fig. 3. The nontetrahedral (additional) coordination of water molecules, which is reflected usually as a separate maximum in $g_{OO}(r,\Omega)$ at the interstitial separations of about 3.2–4.4 Å has been marked in Fig. 3 with A.

First examining the *tetrahedral* coordination in the local water structure, we focus on the dominant maxima of

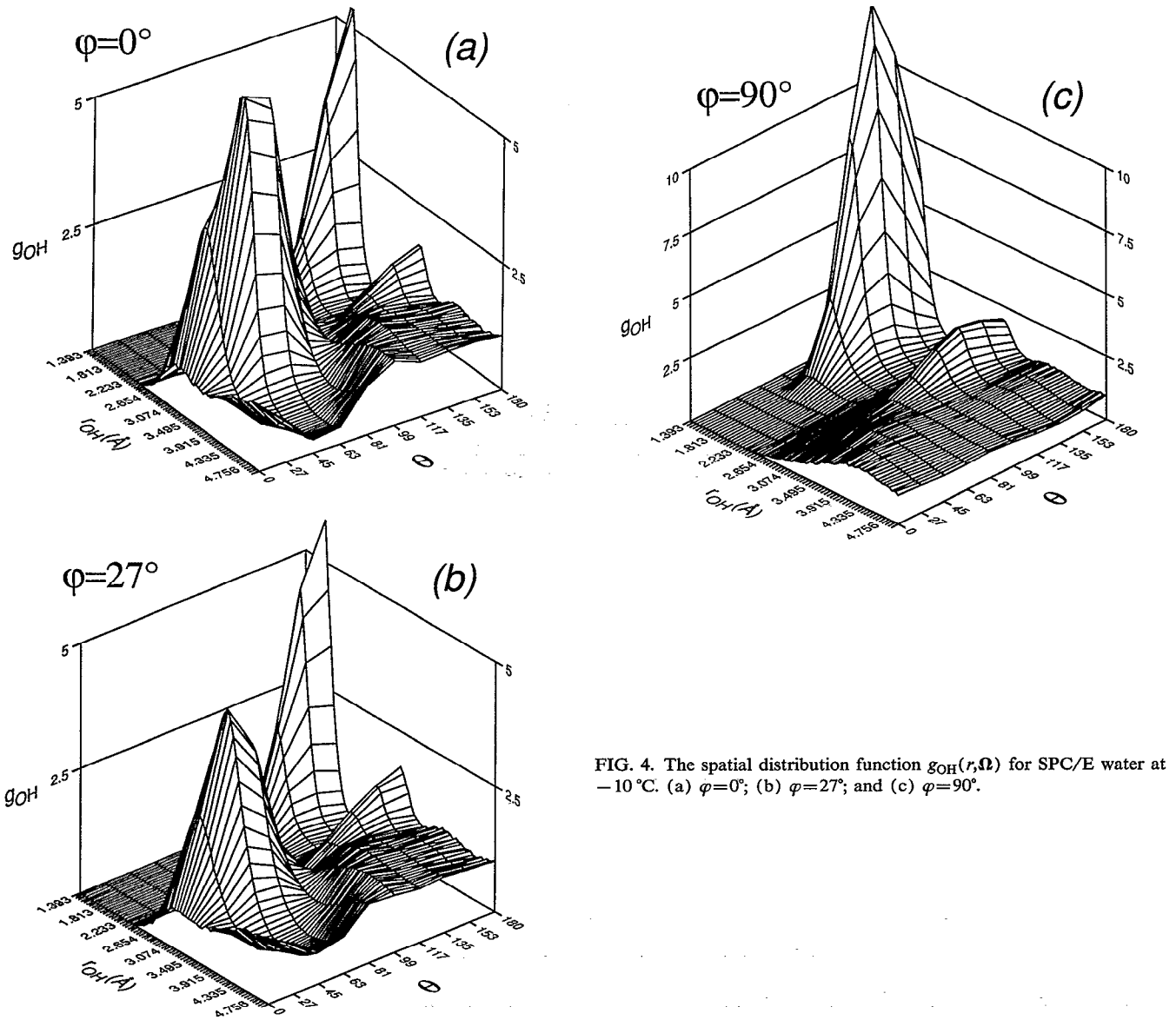

FIG. 4. The spatial distribution function $g_{OH}(r,\Omega)$ for SPC/E water at −10 °C. (a) $\varphi=0°$; (b) $\varphi=27°$; and (c) $\varphi=90°$.

the nearest neighbors, the sharp maximum in $g_{OO}(r,\Omega)$ at $r\approx 2.7$ Å and small θ [Fig. 3(a), plane of the molecule] and the broad maximum at the same separations and large θ [Fig. 3(c), plane of lone-pair electrons]. These maxima reflect the distributions of the oxygen atoms of molecules which, respectively, accept and donate the hydrogen atoms in H bonds with the central (reference) molecule. Unlike the first maximum in $g_{OO}(r)$, the corresponding (four) maxima in $g_{OO}(r,\Omega)$ are very well defined and can be easily integrated to give an average coordination number for the immediate H-bonded neighbors in the local tetrahedral network. This number is 4.0 at −10 °C. We point out that although the chosen interaction potential SPC/E utilizes only *three* atomic interaction sites (it does not explicitly include lone-pair sites), the simulated liquid exhibits a very strong tendency for local tetrahedral packing. At the same time, the nonequivalence (in the principal frame) of molecules donating hydrogen atoms in H bonds with the central molecule, and molecules accepting H bonds from its central partner, is very obvious in $g_{OO}(r,\Omega)$; the distribution of donor molecules is much broader (see Fig. 3). Again, all these important features of the local order in liquid water, real or simulated, cannot be demonstrated from the traditional one-dimensional RDF $g_{OO}(r)$.

We now turn our attention to *temperature* effects in the topology of the tetrahedral network of H bonds. The average number of nearest neighbors in the network has been computed at 25 and 100 °C [by integrating over the appropriate maxima in the corresponding $g_{OO}(r,\Omega)$] and the results indicate that the network coordination number 4.0 does not depend on the temperature in the system (at least over the range −10–100 °C). In order to compare the average spatial positions of the nearest neighbor molecules, we have employed a fixed separation projection of the $g_{OO}(r,\Omega)$, namely, $r_{OO}=2.71$ Å (see Fig. 5). We see in Fig. 5 that the arrangement of the four nearest neighbors in the average local structure in water is sensitive to temperature variations. Although the peaks in the pair-density distributions undergo considerable broadening at 100 °C, the maximum of the first-neighbor acceptors does not change appreciably in its angular coordinates; it remains at $\varphi_{max}=0°$ or 180°. (plane of the molecule) and $\theta_{max}\approx 53°$.

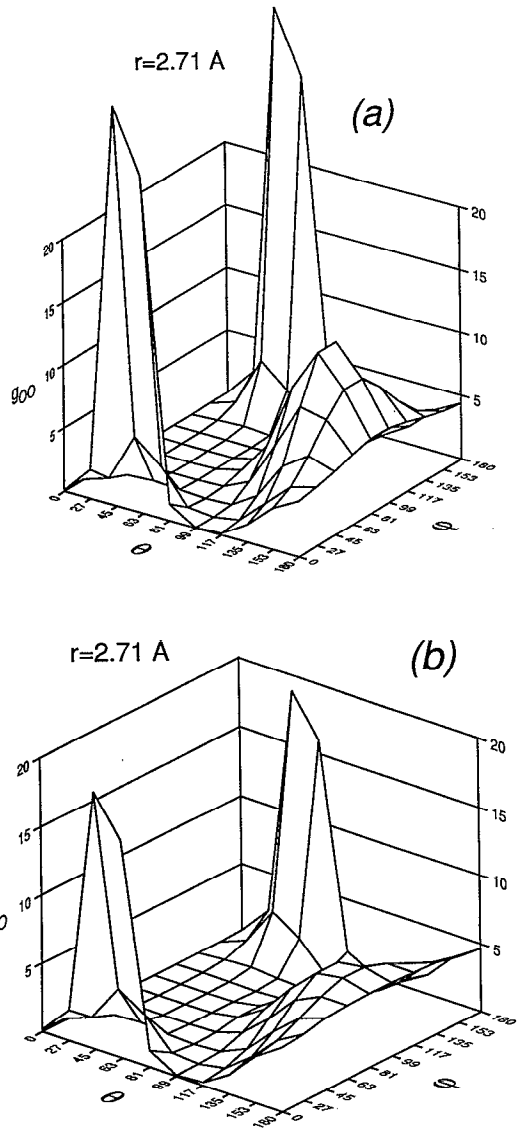

FIG. 5. The spatial distribution function $g_{OO}(r,\Omega)$ at $r=2.71$ Å. (a) $T=-10$°; (b) $T=100$ °C.

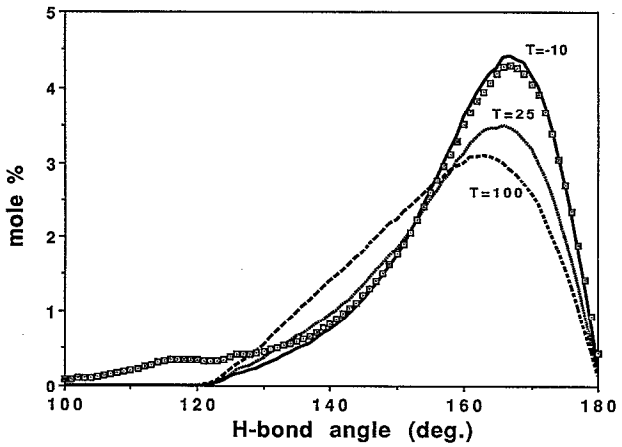

FIG. 6. The distribution of H-bond angles in the tetrahedral network. The solid, dotted, and dashed lines are the results at −10, 25, and 100 °C, respectively. The squares reflect the distribution for all H-bonded pairs at −10 °C.

This implies that the H-bond accepting neighbors retain their near perfect tetrahedral locations even at high temperatures. In contrast, the distribution of H-bond donors (with its maximum in the plane of the lone-pair electrons) is substantially shifted at 100 °C toward the principal Z axis, or larger θ (with θ_{max} at about 150°). Thus, the nearest-neighbor donors prefer to align more along the dipole axis of the central molecule at high temperatures. For comparison, at −10 °C, their maximum in $g_{OO}(r,\Omega)$ occurs at about 130°, while in the perfect tetrahedral assembly $\theta_{max}=125.3$°.

In our structural analysis, we have also considered the statistical distributions of H-bond angles. As is standard practice,[17] we have defined the H-bond angle α as the OH···O angle. However, we have made two unique determinations of the distribution of α. In the first, only those pairs of molecules which belong to the network structure, i.e., which form the distinct first maxima in $g_{OO}(r,\Omega)$ (marked as 1 in Fig. 3), have been selected. In the second, all the pairs with the energy less than or equal to −9.4 kJ/mol (the typical threshold of H bonding[17]) have been included. The results are given in Fig. 6.

Comparing the distribution of H-bond angles for the nearest neighbors of the network with the distribution for all H-bonded pairs (using the same criterion of H bonding as in Ref. 17), we observe that they are virtually identical for angles larger than 130°. At the same time, the shoulder clearly evident below 120° in the data from all H-bonded pairs is missing in the network distributions. This missing shoulder would suggest that the tetrahedral network in the average local structure in water does not contain local segments with small OH···O angles. It is also apparent that there must be some pairs of molecules in the liquid which interact strongly, but which are not tetrahedrally coordinated (hence not H bonded in a geometrical sense). From our statistical distributions, we were then able to compute the average H-bond angle $\langle\alpha\rangle$ in the tetrahedral network. Our estimates are included in Table II and we remark that these values are larger, by about 3°, than the average H-bond angles determined for all H-bonded pairs at these temperatures. This fact again indicates that the tetrahedral network of H bonds in water possesses more linear geometry than is perhaps implied by a simple energetic H-bond analysis.

We now briefly shift our discussion to the coordination of more distant neighbors in the tetrahedral network of H bonds, i.e., those for which the function $g_{OO}(r,\Omega)$ clearly demonstrates further tetrahedral correlations (denoted in Fig. 3 as 2 and 3). Although it was difficult to estimate exactly from our data the average numbers of these more remote network neighbors [because of the lack of clearly delimited peaks in $g_{OO}(r,\Omega)$ at large separations], we have, nevertheless, extracted the average radial positions for the second and the third tetrahedral maxima. In Table III, we compare these direct structural data with the corresponding theoretical estimates given by Rice and co-workers in

TABLE II. Parameters of the local order in SPC/E water.

	Tetrahedral coordination		Additional coordination	
T (°C)	$\langle\alpha\rangle$	N^a	$\langle\alpha\rangle$	$N(N^-+N^+)^b$
−10	161°	4.0	118°	0.80 (0.50+0.30)
25	159°	4.0	117°	0.86 (0.52+0.34)
100	156°	4.0	118°	0.98 (0.56+0.43)

[a]N is the coordination number.
[b]N^- and N^+ are contributions to the coordination number due to neighbors with negative and positive interaction energies, respectively, with the central molecule (as discussed in Sec. IV B).

their work on the RNM.[15] It can be seen that the overall agreement is rather good, although our average separations for the second and the third neighbors in the tetrahedral network exhibit temperature dependencies opposite to those predicted by the RNM. In general, our simulation results appear to support the structural model of a continuous tetrahedral assembly in the local water structure. Of course, these interparticle correlations are not long ranged (the tetrahedral network of H bonds in liquid water will extend only a few molecular diameters) and nor are they long lived.

So far we have focused only on the local tetrahedral packing of the oxygen sites in liquid water as evident in $g_{OO}(r,\Omega)$. In order to provide further insights into the network of H bonds in liquid water, we have also considered the spatial distribution of O–H correlations. The corresponding distribution function $g_{OH}(r,\Omega)$ at −10 °C is shown in Fig. 4. We immediately see that it provides a remarkably rich picture of the local density of hydrogen atoms. We find that the two peaks due to H atoms associated with the same donor molecule ($r_{OH}=1.71$ Å and $r_{OH}=3.28$ Å) have their maxima at $\varphi_{max}=90°$, which implies that these donor molecules prefer to lie in the plane of the lone-pair electrons of the central molecule. These maxima also possess approximately the same $\theta\approx135°$ [see Fig. 4(c)], although the more distant hydrogen peak (at a separation of about 3.28 Å) appears to be much flatter with respect to the angular coordinates. Another interesting feature in Fig. 4 is that the peaks associated with the two hydrogen atoms of the H bond accepting neighbor, collapse into a single featureless maximum centered at $r_{OH}=3.40$ Å, $\theta\approx50°$, and $\varphi\approx0°$ (direct integration of this peak yields exactly 2.0), implying that a variety of orientations is possible for these H-bonded neighbors.

TABLE III. Average separations in Ångstroms for the first, second, and third neighbors in a continuous tetrahedral network.

	First neighbors		Second neighbors		Third neighbors	
T (°C)	MD	RNM[a]	MD	RNM[a]	MD	RNM[a]
−10	2.71	2.82	4.38	4.41	5.33	5.31
25	2.72	2.83	4.38	4.40	5.38	5.29
100	2.73	2.86	4.39	4.37	5.40	5.21

[a]From Ref. 15.

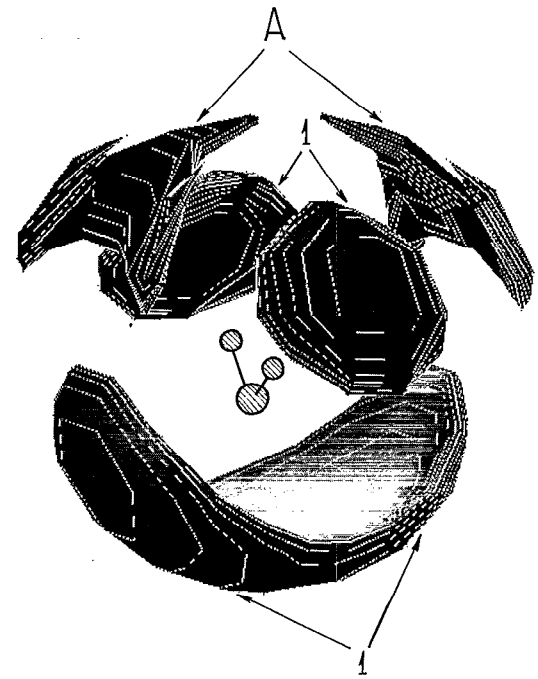

FIG. 7. A three-dimensional map of local oxygen density in liquid water at 25 °C. The isosurface for $g_{OO}(r,\Omega)=1.5$ is shown. The central molecule has been included to define the local frame. A and 1 are the same as in Fig. 3.

It is not difficult to show that $g_{OO}(r,\Omega)$ and $g_{OH}(r,\Omega)$ provide an effective and simple route for characterizing the average geometry of the local order in liquid water. Indeed, given the spatial distributions of O and H sites, estimates for all average parameters (both radial and angular) can be extracted directly from the coordinates of the maxima in $g_{OO}(r,\Omega)$ and $g_{OH}(r,\Omega)$. Thus, if the average H-bond angle in the tetrahedral network is desired, we immediately obtain from the corresponding pair-density peaks a value of about 160° (at −10 °C), which is very close to the value of $\langle\alpha\rangle$ of 161° derived above from I(instantaneous) configurations.

It is well documented[2,4] that the average coordination number in liquid water is substantially larger than the number of the immediate tetrahedral neighbors 4.0, although no direct evidence exists to confirm whether this fact reflects fluctuations in distributions of more remote (second, third,...) neighbors of the tetrahedral network, or an additional nontetrahedral assembly in some local surroundings. It follows from our simulation data that the unfolded OO distribution $g_{OO}(r,\Omega)$, with its distinct maximum at interstitial separations, strongly supports the latter type of local ordering between the first and second tetrahedral coordination shells as being dominant. To help further clarify this point, we have plotted in Fig. 7 a full three-dimensional local density map for oxygen atoms (the surfaces reflect an oxygen density of 1.5 times that of the bulk) at 25 °C. Both the immediate tetrahedral neighbors and the additional coordination can be seen. We note that the interstitial particles appear confined to the region $0<\theta<\pi/2$ (i.e., the upper hemisphere in the principal frame)

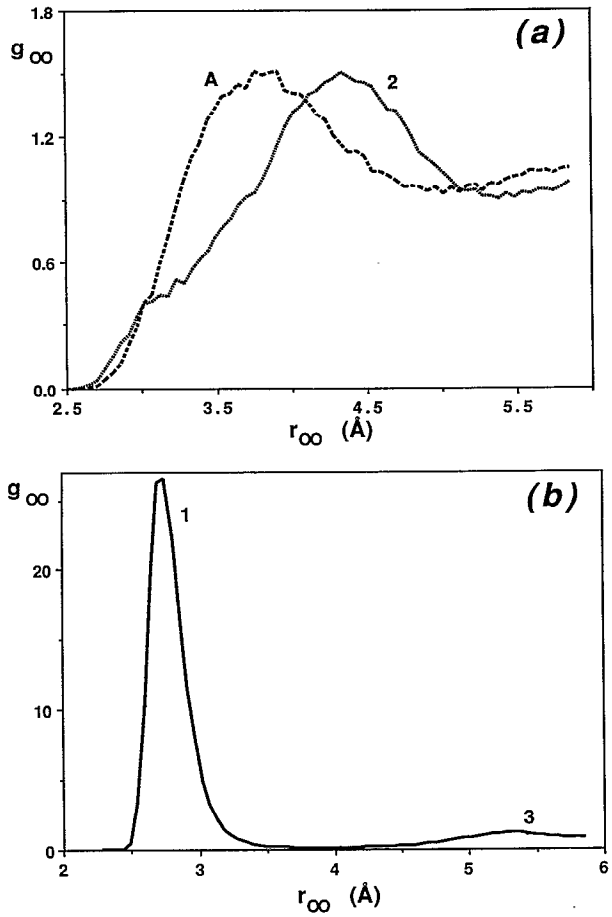

FIG. 8. One-dimensional "slices" of $g_{OO}(r,\Omega)$ at $-10\,^{\circ}C$. The solid, dotted, and dashed lines represent ($\theta=63$, $\varphi=0°$), ($\theta=0$, $\varphi=0°$), and ($\theta=27$, $\varphi=90°$), respectively. 1, 2, 3, and A are the same as in Fig. 3.

with φ close to $\pm 90°$. The principal question to ask at this point is, does this maximum represent correlations in a topologically altered H-bonded network which is nontetrahedral (say in four-member rings), or does it reflect a specific interstitial fraction of water molecules? In the next section, we attempt to address this question in some detail.

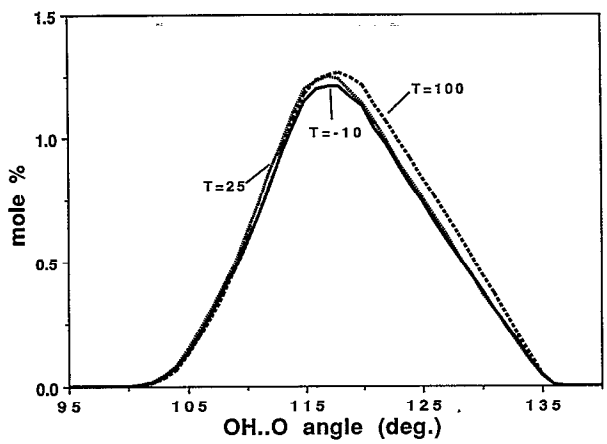

FIG. 9. The distribution of OH···O angles for the additional coordination. The solid, dotted, and dashed lines are the same as in Fig. 6.

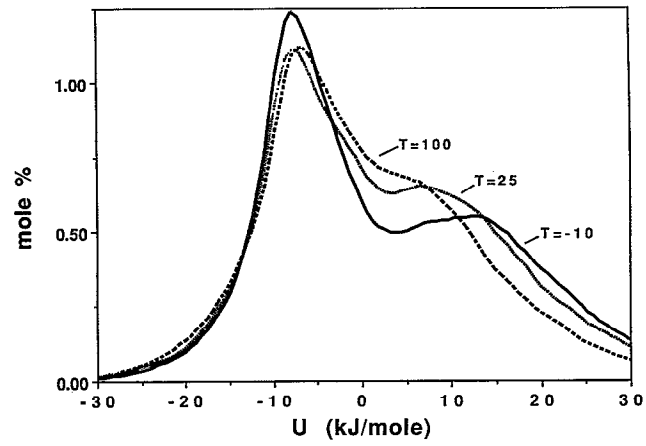

FIG. 10. The distribution of pair energies for the additional coordination. The solid, dotted, and dashed lines are the same as in Fig. 6.

B. Interstitial maximum in $g_{OO}(r,\Omega)$—full coordination number in water

As a first step, we have isolated and integrated the additional (A) maximum in $g_{OO}(r,\Omega)$ over the appropriate spatial coordinates in order to obtain the average number of molecules involved in this coordination. In particular, an outer integration boundary of 4.4 Å was adopted for the radial coordinate (in an attempt to account for all the nontetrahedral neighbors which are displaced closer than the average second tetrahedral neighbor). Figure 8(a) demonstrates typical one-dimensional slices of $g_{OO}(r,\Omega)$ through the additional (nontetrahedral) maximum and the second (tetrahedral) maximum; the slice through the first and the third tetrahedral maxima is shown for comparison in Fig. 8(b). Coordination numbers due to these nontetrahedral neighbors can be found in Table II and, unlike the numbers of the nearest tetrahedral neighbors, they appear to change with the temperature. Given the data in Table II, we can now establish *average full coordination numbers* in liquid SPC/E water of 4.80, 4.86, and 4.98 at -10, 25, and 100 °C, respectively. We remark that more traditional values for the coordination numbers in water of 4.4–4.5 from $g_{OO}(r)$ can be easily recovered from our data by truncation of the interstitial distribution at 3.4–3.5 Å. Whereas this separation corresponds to the *first minimum* in $g_{OO}(r)$, it nonetheless coincides with a *local maximum* in $g_{OO}(r,\Omega)$ for certain values of θ and φ.

In order to further characterize the structure at these interstitial separations, we have selected those molecular pairs which contribute to this local maximum in $g_{OO}(r,\Omega)$ (as defined in Fig 8) and have accumulated their pair energies and OH···O angles. The angular distributions obtained are shown in Fig. 9 and pair-energy distributions are plotted in Fig 10 for all temperatures studied; the average OH···O angles $\langle\alpha\rangle$ are included in Table II. It can be seen in Figs. 9 and 10 that while the angular distributions

for these interstitial neighbors are single peaks which appear rather insensitive to temperature, their pair-energy distributions are clearly bimodal, with one peak occurring at negative energies and a smaller second maximum evident at positive values. This fact is significant in that it indicates that at least two different types of intermolecular ordering may exist at the interstitial separations of 3.2–4.4 Å. Moreover, the relative population of these apparent subfractions also appears sensitive to the temperature.

By approximating the bimodal pair-energy distributions with the sum of two Gaussians, we were able to determine the relative contributions of the two subfractions allowing us to compute the average number of molecules in each. These results can be found in Table II. It follows from Table II that *each* of these subfractions "hidden" in the interstitial maximum of $g_{OO}(r,\Omega)$ accounts for roughly 10% of all neighbors in the first (full) coordination sphere (at 25 °C,[11] and 7% for the negative and positive pair-energy peaks, respectively). Given ring statistics obtained in previous studies (Vol. 7 of Ref. 1 and Refs. 4, 27 and 28), it can be shown that the mole fraction of diagonal partners in four-membered rings in liquid water is approximately 5%–7%; this seems to suggest that one of the peaks in our pair-energy distributions, namely, that at positive energy, is related to a diagonal correlation in local arrangements which could be identified as four-membered rings. We recall that the average separation for this diagonal correlation, as it follows from quantum-chemical calculations,[29,30] is about 3.4–3.9 Å, which agrees well with the position of the local density maximum in $g_{OO}(r,\Omega)$. It also follows from these previous calculations[29,30] that due to stereoelectronic restrictions in small connected rings, the diagonal neighbors must have relative orientations similar to that shown in Fig. 11(a). In this figure, the molecules lie in essentially perpendicular planes and the dipole vector of one of the molecules [the small arrow in Fig. 11(a)] and the principal X axis of the other form an angle of 30°. The energy of 7.0 kJ/mol for such a diagonal arrangement compares well with the average position of the positive peak in our distribution of pair energies. (To be consistent with our definition of the "additional" coordination shown in Fig. 7, we have required $r_{OO}=3.3$ Å, $\theta=45°$, and $\varphi=0°$ for this pair.) Together, the direct structural data and our related analysis of pair energies confirm the existence of small rings in the H-bonded network in liquid water, and in accord with the topological analysis of network distortions given by Sceats and Rice (Vol. 7 of Ref. 1), we suggest that small H-bonded rings (nontetrahedral coordination) and the tetrahedral network represent unique fractions in the liquid structure. We again point out that neighbors that are part of small ring structures and which are closer to the central molecule than the second tetrahedral H-bonded neighbors are included in our average full coordination numbers.

Now turning our attention to the distribution of the negative pair energies, we remark that this peak is distinctly sharper than the peak due to strongly repulsive diagonal pairs in small rings. It is important to note that the magnitude of the distribution average (−7.8 kJ/mol at 25 °C) is lower than accepted energetic thresholds of H bonding in liquid water [typically −9.4—−10.0 kJ/mol (Refs. 17 and 31)], yet it is also clear that some of these nontetrahedral neighbors would be energetically classified as H-bonded neighbors. We suggest that this feature of the negative pair-energy distribution reflects the existence of a distinct fraction in water which interacts strongly with the central molecule, but which would not usually be seen as being H bonded. In Figs. 11(b) and 11(c), we have shown two of the interstitial pairs (where the dipole axis of interstitial neighbor coincides with the separation vector) which probably contribute to the distribution at negative pair energies. Indeed, if $r_{OO}=3.3$ Å, $\theta=45°$, and $\varphi=0°$, pair energies of −7.0 and −6.3 kJ/mol are obtained for the perpendicular and the parallel arrangements, respectively, which agree with the position of the negative peak. We mention also that energies as small as −15 kJ/mol can be obtained by simply reducing θ.

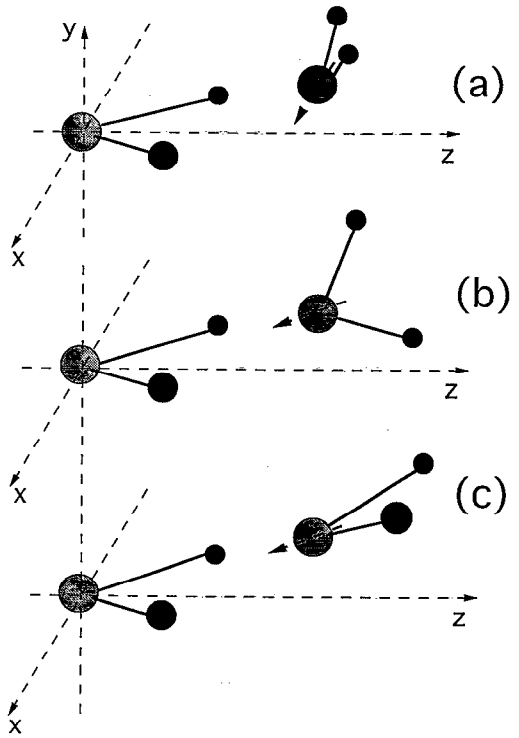

FIG. 11. Some examples of the additional coordination geometry (as discussed in Sec. IV B).

Finally, in order to more fully understand the implications of the local structure in liquid water, we have undertaken a visual analysis of particle trajectories. In general, the animation of small sets of configurations indicates an interesting link between the interstitial molecules and those neighbors in the local network, which leave their tetrahedral positions in the process of thermal motion to fill local potential wells in the cavities of a fluctuating network. Detailed analysis of the molecular dynamics of different water fractions and the connection of the dynamics to various spectra (resolved in local frame) will be given in a future article.[20]

Concluding our structural discussion, we would add that the SDF $g_{OO}(r,\Omega)$ can be easily converted into a potential of mean force $\omega_{OO}(r,\Omega) = -(kT)^{-1} \ln[g_{OO}(r,\Omega)]$. Such a potential would represent the effective interaction resulting from the average over all orientations of the individual molecules and could be applied using Langevin dynamics to the study of long-time hydrodynamic processes in water.

V. CONCLUSIONS

In this article, we have reported results from MD simulations of liquid water at -10, 25, and 100 °C performed with the SPC/E pair potential. We have examined the spatial distribution functions, namely, $g_{OO}(r,\Omega)$ and $g_{OH}(r,\Omega)$, and have applied them to an analysis of equilibrium structure in liquid water. One of the principal aims in this work has been to develop a practical, yet systematic, approach with which to study the average local structure in a complex liquid system.

Using the information directly available from $g_{OO}(r,\Omega)$ and $g_{OH}(r,\Omega)$, we have analyzed the local H-bonded tetrahedral structure in liquid water and have determined that the value of the network coordination number is 4.0 and does not depend on temperature. As expected, the average H-bond angle in the tetrahedral network structure was found to be more linear than the average H-bond angle for all energetically H-bonded pairs. Examining the structure in $g_{OO}(r,\Omega)$ at different temperatures, we were also able to clarify that those nearest neighbors which donate hydrogen atoms in H bonds with the central molecule tend to prefer to align along the dipole axis of the central particle at high temperatures, while the H-bond accepting neighbors remain very close to their ideal tetrahedral positions. One of the most striking features of $g_{OH}(r,\Omega)$ was that the distributions associated with the two hydrogen atoms of the H-bond accepting neighbors collapse (in the local frame) into a single maximum, which implies that these network partners can be found in a variety of possible orientations.

We have examined in detail the local pair-density maximum in $g_{OO}(r,\Omega)$ at the interstitial separations of about 3.2–4.4 Å. This maximum is clearly observed at nontetrahedral positions in the local frame. Furthermore, we have carried out an integration of this local maximum and have obtained the additional coordination number due to these neighbors. Addition of this value to the network coordination number yields an average full coordination number of 4.8–5.0 in liquid water over the temperature range -10–100 °C. A pair-energy analysis was performed and it revealed that two different types of molecular ordering appear to contribute to the interstitial maximum—formation of small ring structures in the network of H bonds (with nontetrahedral coordination of the diagonal neighbors), and a separate fraction that interacts strongly with the central molecule (although the *average* dimerization energy in this separate fraction does not exceed the usual threshold of H bonding in liquid water).

Clearly, the present approach based on the spatial distribution functions could be extended to help analyze the local structure in liquid systems with complex behavior. We remark that work is currently underway to examine H bonding in liquid alcohols. We also hope to apply spatial charge-density maps, corresponding to $g(r,\Omega)$, in a detailed investigation of proton screening in liquids; our recent computer simulation study of proton chemical shifts in liquid water[32] has indicated an important and nontrivial effect due to particles beyond the first coordination shell.

ACKNOWLEDGMENTS

We are grateful for the financial support of the Natural Sciences and Engineering Research Council of Canada. I.M.S. also wishes to thank Professor F. Stillinger and Professor G. Walrafen for useful discussions.

[1] *Water—A Comprehensive Treatise*, edited by F. Franks (Plenum, New York, 1972–79), Vols. 1–8.
[2] D. Eisenberg and W. Kauzmann, *The Structure and Properties of Water* (Oxford University, New York, 1969).
[3] P. A. Giguere, J. Raman Spectrosc. **17**, 341 (1986).
[4] C. Corongiu and E. Clementi, J. Chem. Phys. **97**, 2030 (1992).
[5] A. K. Soper and M. G. Phillips, Chem. Phys. **107**, 47 (1986).
[6] I. M. Svishchev and P. G. Kusalik, Physica A **192**, 628 (1993).
[7] I. M. Svishchev and P. G. Kusalik (to be published)
[8] J. D. Bernal and R. N. Fowler, J. Chem. Phys. **1**, 515 (1933).
[9] J. Morgan and B. E. Warren, J. Chem. Phys. **6**, 666 (1938).
[10] O. Ya. Samoilov, *Structure of Aqueous Electrolyte Solutions and the Hydration of Ions* (Consultants Bureau, New York, 1965).
[11] A. Ben-Naim, *Water and Aqueous Solutions* (Plenum, New York, 1974).
[12] A. H. Narten, M. D. Danford, and H. A. Levy, Discuss. Faraday Soc. **43**, 97 (1967).
[13] J. Lennard-Jones and J. A. Pople, Proc. R. Soc. London Ser. A **205**, 155 (1951).
[14] J. A. Pople, Proc. R. Soc. London Ser. A **221**, 498 (1954).
[15] M. G. Sceats, M. Stavola, and S. A. Rice, J. Chem. Phys. **70**, 3927 (1979).
[16] A. C. Belch, S. A. Rice, and M. G. Sceats, Chem. Phys. Lett. **77**, 455 (1981).
[17] W. L. Jorgensen *et al.*, J. Chem. Phys. **79**, 926 (1983).
[18] W. L. Jorgensen, J. Chem. Phys. **77**, 4156 (1982).
[19] H. J. C. Berendsen, J. R. Grigera, and T. P. Straatsma, J. Phys. Chem. **91**, 6269 (1987).
[20] I. M. Svishchev and P. G. Kusalik, J. Phys. Chem. (to be published).
[21] D. J. Evans and J. P. Morriss, *Statistical Mechanics of Nonequilibrium Liquids* (Academic, San Diego, 1990).
[22] D. Fincham and D. M. Heyes, Adv. Chem. Phys. **63**, 493 (1985).
[23] M. P. Allen and D. J. Tildesley, *Computer Simulations of Liquids* (Oxford University, Oxford, 1987).
[24] P. G. Kusalik, J. Chem. Phys. **93**, 3520 (1990).
[25] D. J. Evans and J. P. Morriss, Comput. Phys. Rep. **1**, 297 (1984).
[26] M. Rami Reddi and M. Berkowitz, Chem. Phys. Lett. **155**, 173 (1989).
[27] R. S. Speedy, J. D. Madura, and W. L. Jorgensen, J. Phys. Chem. **91**, 909 (1987).
[28] K. A. Motakabbir and M. Berkowitz, J. Phys. Chem. **94**, 8359 (1991).
[29] J. Del Bene and J. A. Pople, J. Chem. Phys. **52**, 4858 (1972).
[30] B. R. Lentz and H. A. Scheraga, J. Chem. Phys. **58**, 5296 (1973).
[31] F. H. Stillinger and A. Rahman, J. Chem. Phys. **60**, 1545 (1974).
[32] I. M. Svishchev and P. G. Kusalik, J. Am. Chem. Soc. (in print).